Formation and erosion of sediment cover in an experimental bedrock-alluvial channel

Rebecca Hodge[1], Trevor Hoey[2], Georgios Maniatis[2,3] and Emilie Leprêtre[4]

[1] Department of Geography, Durham University, Durham, UK

[2] School of Geographical and Earth Sciences, University of Glasgow, UK

[3] School of Computing Science, University of Glasgow, UK

[4] Suez Environment and University of Montpellier, France

Accepted by Earth Surface Processes and Landforms

Abstract

Sediment grains in a bedrock-alluvial river will be deposited within or adjacent to a sediment patch, or as isolated grains on the bedrock surface. Previous analysis of grain geometry has demonstrated that these arrangements produce significant differences in grain entrainment shear stress. However, this analysis neglected potential interactions between the sediment patches, local hydraulics and grain entrainment. We present a series of flume experiments that measure the influence of sediment patches on grain entrainment. The flume had a planar bed with roughness that was much smaller than the diameters of the mobile grains. In each experiment sediment was added either as individual grains or as a single sediment pulse. Flow was then increased until the sediment was entrained. Analysis of the experiments demonstrates that: 1) for individual grains, coarse grains are entrained at a higher discharge than fine grains; 2) once sediment patches are present, the different in entrainment discharge between coarse and fine grains is greatly reduced; 3) the sheltering effect of patches also increases the entrainment discharge of isolated grains; 4) entire sediment patches break-up and are eroded quickly, rather than through progressive grain-by-grain erosion, and 5) as discharge increases there is some tendency for patches to become more elongate and flow-aligned, and more randomly distributed across the bed. One implication of this research is that the critical shear stress in bedrock-alluvial channels will be a function of the extent of the sediment cover. Another is that the influence of sediment patches equalises critical shear stresses between different grain sizes and grain locations, meaning that these factors may not need to be accounted for. Further research is needed to quantify interactions between sediment patches, grain entrainment and local hydraulics on rougher bedrock surfaces, and under different types of sediment supply.

1. Introduction

Semi-alluvial channels are identified by their predominantly bedrock channel boundaries and partial alluvial cover (Turowski *et al.*, 2008). The total extent of sediment cover within a semi-alluvial channel is a function of the sediment supply relative to transport capacity, although the exact form of this relationship is debated (Sklar and Dietrich, 2004; Turowski *et al.*, 2007; Chatanantavet and Parker, 2008; Hodge and Hoey, 2012). The spatial arrangement of the sediment cover within the channel is in turn the result of interactions between the bedrock topography, channel hydraulics and sediment transport processes (Hodge *et al.*, 2011; Nelson and Seminara, 2012; Inoue *et al.*, 2014; Johnson, 2014; Zhang *et al.*, 2015). These two factors, the total extent and spatial arrangement of sediment cover, are inter-related in ways that have yet to be investigated. As with alluvial bedforms, sediment patches can develop in response to boundary shape (analogous to 'forced' bars in alluvial literature; Seminara 2010; described as externally controlled by Wohl, 2015) or as a result of the interactions between flow, bedform morphology and sediment transport (equivalent to 'free' bars). To date, emphasis has been on how forced sediment accumulations, whether due to irregular bedrock topography (Turowski and Rickenmann, 2009; Siddiqui and Robert, 2010; Hodge and Hoey, in revision) or large immobile boulders (Carling and Tinkler, 1998; Carling *et al.*, 2002; Chatanantavet and Parker, 2008; Papanicolaou *et al.*, 2012) affect flow and sediment cover. To interpret sediment accumulation and erosion in natural channels (e.g. Hodge and Hoey, in revision) which are always likely to have a component of morphological forcing of sediment cover, understanding of how self-formed 'free' bedforms function in semi-alluvial channels is required.

61 The location of a grain within a semi-alluvial channel can have a significant effect on
62 that grain's critical shear stress (τ_c) and hence the ease with which it is entrained by
63 the flow. Isolated sediment grains on a smooth bedrock surface can have values of
64 τ_c that are an order of magnitude less than comparable grains in an alluvial patch
65 (Hodge *et al.*, 2011). This difference is the result of the differing pocket geometries
66 on grain exposure and pivot angle. Differences in roughness, and hence flow profiles
67 and local shear stress, over the alluvial and bedrock surfaces are also likely to
68 exacerbate differences in grain transport potential (Inoue *et al.*, 2014; Johnson,
69 2014). The spatial pattern of roughness elements in semi-alluvial channels is very
70 variable (Chatanantavet and Parker, 2008; Inoue *et al.*, 2014), complicating attempts
71 to develop empirical relationships for controls over patch development.
72 Consequently, we focus here on sediment patches on planar, relatively smooth,
73 surfaces in order to isolate the effects of grain-scale interactions on patch
74 development and erosion.

75 From the perspective of grain geometry, the distribution of isolated grains and
76 sediment patches across a bedrock surface determines the distribution of τ_c for the
77 population of grains (Hodge *et al.*, 2011), and hence the sediment flux at low
78 discharges. At higher discharges when the applied shear stress (τ) is much greater
79 than τ_c, all sediment will be fully mobile and the range of τ_c is no longer significant.
80 However, the typical lognormal distribution of flow events in a river combined with
81 low values of τ_c for isolated grains means that low flow events can have a more
82 significant impact on the total sediment flux than is the case in alluvial rivers with the
83 same sediment sizes (Lisle 1995; Hoey and Hodge, in prep). Theoretical modelling
84 has demonstrated that by distributing the same amount of sediment cover in different
85 ways (i.e. different proportions of grains in bedrock and alluvial positions) the

resulting average sediment fluxes range from less than to greater than the average sediment flux in a comparable alluvial river (Hoey and Hodge, in prep). An understanding of the development of sediment cover in semi-alluvial channels is therefore necessary in order to predict sediment fluxes in these systems.

There is little empirical data with which to constrain the most likely distributions of sediment cover, however, previous research has identified some first order tendencies. Higher values of τ_c for grains in alluvial patches are likely to produce a net flux of grains from bedrock surfaces to alluvial patches (Nelson and Seminara, 2012). Sediment is thus most likely to form alluvial patches, with only a small fraction of the grains remaining isolated on bedrock surfaces. This pattern is consistent with field sediment tracer data (Hodge *et al.*, 2011). The position and form of alluvial patches will be controlled by both the underlying bedrock topography and interactions between the patch roughness and the local hydraulics (Finnegan *et al.*, 2007; Johnson and Whipple, 2010; Hodge and Hoey, in revision). Alluvial bedforms such as pebble clusters affect the local hydraulics, causing a downstream separation zone and coherent flow structures with well-defined spatial characteristics (Strom and Papanicolaou, 2007; Lacey and Roy, 2008). Similar processes will occur around alluvial patches, amplified by the potential contrast in roughness between bedrock and alluvial regions and the topographic expression of patches on a bedrock surface, so affecting the growth and shape of the patches and local sediment transport. Whether flow conditions are steady or varying, it is unclear how the bedforms interact and whether these interactions are predominantly regenerative (maintaining bedforms of a given size) or constructive (tending to merge bedforms into a smaller number of larger features) (Kocurek *et al*., 2010).

To begin to address the issues raised above, in this paper we present results from flume experiments on the development and erosion of sediment cover on a bedrock surface. We simplify conditions to assess the fundamental process controls over free bedforms, and use uniform channel width, slope and roughness. In each experiment, a fixed volume of sediment was introduced at the upstream end of a flume with a plane bed of constant low roughness, which resulted in sediment patches developing. Once sediment cover had developed, flow was increased at a known rate and the sediment cover was eroded. The aims of the experiments are to: 1) quantify the impact of grain size and position on τ_c, which is recorded by the flow at which different grains are entrained; and, 2) quantify patch geometry and how this changes as patches are eroded. Results are reported from three sets of experiments: Set 1, control experiments using single grains and no sediment patches; Set 2 with a uniform coarse grain size; and Set 3 with different mixtures of two uniform sediments, one coarse and one fine.

2. Methods

Three sets of experiments (Sets 1, 2 and 3; Table 1) were carried out in a 0.9 m wide flume which has a working length of 8 m and maximum flow of 75 l s^{-1}. A flat plywood bed was installed in the flume, with small-scale roughness added by fixing a layer of < 0.5 mm sand to this using varnish. Flume slope was 0.0067 (Sets 1 and 3) and 0.0050 (Set 2). Uniform flow was established throughout the operational section at the start of each run by setting discharge to be close to the sediment transport threshold and adjusting the elevation of the flume tail gate until water depth was constant through the measuring section. Under the initial low flow conditions, flow depths varied from 9 to 40 mm. As flow increased, maximum flow depths were between 50 and 80 mm. Flow properties vary according to the sediment cover on the

bed. With no sediment cover, flows across the experimental range of 8.5 to 40 l s^{-1} had a Froude number between 1.27 and 1.33, and Reynolds number of 9100 to 40300. As sediment patches develop, flow may become subcritical. Under the extreme condition of full sediment cover (which is more cover than seen in the experiments), flows from 5.4 to 33 l s^{-1} have Froude numbers between 0.20 to 0.48 and Reynolds numbers from 5400 to 30300.

Figure 1 outlines the experimental procedure. Set 1 experiments (Table 1) were a control to measure the entrainment threshold for the material used in later experiments when introduced as single, isolated grains. Two very angular sediments (0.2 on the Krumbein roundness scale; Krumbein, 1941) with uniform grain sizes were used for the experiments. Coarse sediment (C) has D_{50}=15 mm and fine sediment (F) has D_{50} = 8.5 mm. In each Set 1 experiment a single, randomly selected, grain was placed on the centreline of the flume ~4 m from the flume entrance and flow was increased until the grain was entrained. Fifty measurements were made, twenty five with each of the fine and coarse grains.

In Set 2 and 3 experiments, a known volume of sediment was introduced at the initial discharge, and allowed to developed patches of sediment cover in the measurement section which extended from 5.5 to 5.8 m along the flume and across the entire width of the flume (a total area of 0.27 m^2, determined by the video camera field of view). Sediment cover in the measurement area was representative of that in the rest of the flume. Furthermore, each experiment was repeated at least three times. The initial discharge was maintained until there was little temporal variation in cover extent, which typically took about 15 min to form. Sediment cover extent ranged from 13% to 23%. Flow was then increased at a rate of 1.2 l s^{-1} per minute until the maximum capacity of the pump was reached to erode the sediment grains and patches. Patch

160 formation and erosion was recorded by vertical video photography. Set 2 consisted
161 of 21 repeat experiments each using 20 kg of coarse sediment C. Set 3 used the
162 sediments C and F mixed in the following proportions (where the numbers refer to
163 the percentage of each size fraction in the mixture): 100C, 75C/25F, 50C/50F,
164 25C/75F, 10C/90F and 100F. Each set 3 experiment used 6 kg of sediment,
165 although the proportion of this that formed sediment patches the measuring section
166 varied between runs. Up to 5 repeats were performed of each experiment in Set 3.

167 Two main approaches were used to analyse the video of the experiments in Sets 2
168 and 3. The first was watching the erosion of the sediment cover, and identifying the
169 time and hence discharge at which isolated grains, and those in patches, were
170 eroded. Isolated grains were defined as being those with contact with ≤ 2 other
171 grains in Set 2, and as one grain diameter from any other grain in Set 3. These
172 different definitions reflect differences in the typical behaviour of the coarse and fine
173 grains. In runs with both coarse and fine grains, patches were classified by grain
174 sizes within the patch (coarse, fine or mixed). The analysis noted the time (and
175 hence discharge), of the first entrainment of isolated grains (defined as three grains
176 moving a distance of one or more grain diameters), and the first break up of a stable
177 alluvial patch. In Set 3, the timing of the entrainment of all grains within the imaged
178 area was also recorded. In both sets grains entering the frame from upstream were
179 ignored.

180 The second analytical approach was to measure the sediment cover and the patch
181 geometry. Stills from the videos of the experiments were analysed using two different
182 methods. In the first, the software ImageJ (http://imagej.nih.gov/ij/index.html) was
183 used to segment automatically the grains from the background using the Trackmate
184 algorithm (Crocker and Grier, 1996). Isolated grains were manually identified, and

their areas calculated by the software. The algorithm results were visually assessed to ensure that grains were being identified correctly. The segmentation algorithm was applied to images of high flows over an empty bed to quantify phantom cover caused by scattered light, and this amount of cover was removed from the total calculated from subsequent images. In the second approach, grains were digitised by manually marking the centre of every grain in the frame, and identifying whether the grain was fine or coarse. Image aberration due to the water surface was not explicitly accounted for because it was possible to visually identify the location of all grains.. All grains within one grain diameter were identified as being members of the same patch, and isolated grains were those that were more than one grain diameter from any neighbouring grain (Figure 1).

The two techniques give comparable estimates of the proportion of sediment cover, with the RMS error between estimates from 65 frames being 0.026.The similarity between the two sets indicates that the automated segmentation techniques are robust. In Set 2 experiments, changes in the proportion of sediment cover were assessed in 142 frames using Image J. In Set 3 experiments, digitisation of grains was carried out on twelve runs; two of each sediment mixture. For each run, frames from one, five and every subsequent five minute interval after the onset of the flow increase were analysed.

A number of patch statistics were calculated from the digitised Set 3 images: dimensions, orientation and Ripley's *K* statistic. Patch dimensions were calculated using the Matlab function regionprops, which fits an ellipse with the same second moments as the patch area (where the second moment of an area reflects the distribution of material within the area), and provides the major and minor axis lengths and major axis orientation. This method takes into account all sediment

within the patch, rather than just at the extremes as a bounding box approach would do, and provides an estimate of patch size that is less sensitive to patch shape. Ripley's *K* statistic is a measure of how points are distributed across a surface, describing whether points are more evenly distributed or more clustered than a random spacing (Hajek *et al.*, 2010; L'Amoreaux and Gibson, 2013). The *K* statistic is calculated at a range of lags in order to identify whether the distribution changes as a function of spatial scale. The statistic is estimated for lag *r* (defined here as a number of grain diameters) using:

$$\widehat{K}(r) = \frac{1}{\widehat{\lambda} N} \sum_{\substack{i=1 \\ i \neq j}}^{N} \sum_{j=1}^{N} w\left(s_i, s_j\right)^{-1} \partial_{ij}(r) \quad [1]$$

(Cressie, 1991; L'Amoreaux and Gibson, 2013) where *N* is the total number of events in the study area, $\hat{\lambda}$ is the density of events in the study area, and s_i, s_j are two different events within the area. The weighting factor $w(s_i,s_j)$ accounts for edge effects and ∂_{ij} serves as a counting function being 1 when the distance between s_i and s_j is ≤ 1, otherwise $\partial_{ij} = 0$. *K* is then re-scaled using:

$$\hat{L}(r) = \left(\widehat{K}(r)/\pi\right)^{0.5} - r \quad [2].$$

A spatially random distribution has $\hat{L}(r) = 0$ and values > 1 indicate more clustering and values < 1 more regular spacing, than a random distribution. A Monte Carlo approach is used to calculate a confidence interval for the K statistic. For each digitised image, 100 datasets with the same number of points as the image, but with the points at random locations are produced. *K* statistics at different spatial lags are calculated for these datasets, and the 2.5th to 97.5th percentile envelope of these lags produces a 95% confidence interval.

3. Results

3.1. Grain entrainment shear stress

Results of the conditions under which grain entrainment occurred are mainly reported in terms of discharge, rather than shear stress. The shallow flow depths relative to the grain size produced non-uniform flow over the sediment patches, meaning that du Boys' approximation of shear stress is not applicable for Sets 2 and 3. However, in Set 1 the single isolated grains did not significantly disrupt the uniform flow in the flume, and so du Boys' approximation is valid. Flows were also too shallow to measure local velocity profiles that could be used to calculate shear stress.

Figure 2 shows the distributions of discharge at which isolated grains and alluvial patches first began to move in experimental Sets 1 and 2. In Set 1, fine and coarse isolated grains move at mean discharges of 5.8 (±0.31) l s^{-1} (one standard error) and 8.3 (±0.81) l s^{-1} respectively. These are equivalent to shear stresses of 0.95 (±0.02) and 1.12 (±0.05) Pa, and dimensionless shear stresses of 0.007 (±0.0002) and 0.004 (±0.0002). These entrainment discharges for the coarse and fine grains are significantly different (t-test, $p = 0.007$).

In Set 2, isolated coarse grains start to move at a discharge of 10 l s^{-1}, with coarse grains in patches beginning to move at a significantly higher discharge of 21 l s^{-1} (t-test, $p < 0.0001$). Entrainment discharges of isolated coarse grains in Set 2 are higher than for isolated coarse grains in Set 1, although this is not statistically significant (t-test, $p = 0.057$). This 20% increase in discharge between Sets 1 and 2 is equivalent to approximately a 10% rise in shear stress (assuming that shear stress is proportional to flow depth and that this scales with $Q^{0.5}$, and remembering that du Boys' approximation cannot be applied to Set 2).

Distributions of entrainment shear stresses from Set 3 are shown in Figure 3. In these boxplots, data from the different replicate runs are amalgamated. Such amalgamation is supported by application of the Kruskal-Wallis test, which was used to compare the entrainment discharge for grains of the same size and in the same location between different replicates. In 6 out of the 23 combinations of sediment mixture and grain position, there was no significant difference ($p > 0.05$) between any of the different replicate runs. In 14 of the other combinations, application of Tukey-Kramer revealed that within each set of replicates, only one distribution was significantly different to the other ones.

In Set 3, across all sediment mixtures, fine grains in both isolated and patch locations start to be entrained at a discharge of around 9 l s^{-1} (Figure 3). Coarse grains in isolated and patch locations show a similar behaviour when there is up to 50% fines in the sediment mixture, and this behaviour is comparable to the behaviour of the coarse grains in Set 2. However, when more than 50% of the mixture is fine sediment, coarse isolated grains and coarse patches start to be entrained at higher discharges. Figure 3 also shows the variation in initial entrainment between replicate runs. Across all sediment mixtures, isolated fine grains have initial entrainment over a range of 3.6 l s^{-1}, whereas for coarse isolated grains there is more variability and the range is 7.6 l s^{-1}. There is most variability in the initial entrainment from fine and coarse patches, with ranges of 19.7 and 19.6 l s^{-1}. Initial entrainment from mixed patches has similar values and range to that of course isolated grains. Such variability in initial motion is consistent with that observed in the field by Richardson *et al.* (2003).

Consolidating the above interpretation (Figure 3), the Kruskal-Wallis test indicates a significant difference ($p < 0.05$) between the minimum discharges for different grain

sizes and positions in runs 100C/0F, 10C/90F, 50C/50F and 25C/75F. Additional use of the Tukey-Kramer test confirms that the main differences are between patch and isolated grains. An alternative grouping of the data by grain size and location, and hence comparison between sediment mixtures, showed that the only significant variation in minimum discharge with sediment mixture is for coarse isolated grains.

In Set 3, grain size and location affects the discharge (value and variability) at initial grain entrainment. In contrast, the mean discharge at which grains are entrained is less variable between different grain sizes and locations. As before, there is most variation in the replicate runs for grains in fine and coarse patches. Grains in these patches are also the most affected by the composition of the sediment mixture; as the percentage of fines increases, the mean entrainment shear stress for grains in fine and coarse patches decreases and increases respectively.

Application of the Kruskal-Wallis test to the full distributions of entrainment discharges for all mobile grains revealed that for each sediment mixture, there were significant differences between grains in different locations ($p \leq 0.02$). Further analysis with Tukey-Kramer revealed that in all cases the significant differences were between grains in isolated and patch positions. For each sediment mixture, there was no significant difference between the distributions of entrainment discharge for coarse and fine isolated grains if both were present. For each mixture there was also no significant difference between grains in the various types of patches, with the exception of the fine and mixed patches in 10C/90F.

The analysis of sediment entrainment has demonstrated that: 1) the impact of grain size on entrainment discharge become less important once there are sediment patches present; 2) the presence of sediment patches increases the entrainment

306 discharge for isolated grains as well as for patch grains, indicating the impact of
307 patches on hydraulics; 3) grain location has a greater impact on the minimum
308 entrainment discharge than on the mean; and 4) fine and coarse patches become
309 relatively less and more stable respectively as the proportion of fines in the sediment
310 mixture increases.

311 ### 3.2. Erosion of sediment cover

312 The extent of sediment cover at steady state was an average of 22.4 (±0.24)% (one
313 standard error) in Set 2 experiments and 15.6 (±0.6)% in Set 3 experiments. In Set 3
314 runs, over 80% of initial sediment cover was in patches. This proportion decreased
315 as the sediment was eroded. In Set 3, the extent of sediment cover did not vary
316 systematically with the proportions of coarse and fine sediment, although the most
317 extensive covers were produced by mixtures of coarse and fine sediment. As
318 discharge increased, erosion decreased the areal extent of sediment cover. In Set 2
319 experiments, the total area occupied by patches remained approximately constant
320 until a discharge of ~ 20 l s^{-1}, after which the area decreased approximately linearly.
321 Erosion of isolated grains commenced as soon as discharge began to increase, and
322 no isolated grains remained once discharge exceeded 25 l s^{-1}. Set 3 experiments
323 show a similar overall pattern, although the areal extent of patches begins to
324 decrease as soon as the discharge begins to rise rather than only after a threshold
325 value as in Set 2. As in Set 2, isolated grains in Set 3 are mostly removed by a
326 discharge of 25 l s^{-1}. In both Set 2 and Set 3, there is variability between runs,
327 reflecting specific grain arrangements that occurred as the patches developed.

328 ### 3.3. Sediment patch geometry

329 The digitised grain data from the Set 3 experiments show how patch geometry
330 (number, area, orientation and elongation) changed during erosion (Figure 5). As the

patches are eroded, there is a systematic decline in the number of patches (Figure 5a), and the remaining patches become more flow-aligned (Figure 5c). In most runs there is a concurrent decrease in patch area (Figure 5b), but this decrease is less consistent between the different runs. Finer sediment mixtures tend to have more, smaller, patches. Average patch elongation (major:minor axis length, Figure 5d) has an initial value of 2.4 in all runs. As erosion occurs, elongation generally remains between 2 and 3, apart from a small number of runs in which significantly more elongate patches develop when discharge > 20 l s^{-1}.

Within-run analysis of these properties (Figure 6) shows considerable variability on top of the trends in Figure 5. In some cases there is an observable change in the distribution of patch properties as discharge increases and patches are eroded (Figure 6a and b); and in other cases the distributions remain the same (Figure 6c). In most runs the size of the largest patch decreases with increasing discharge. Changes in the distribution of patch orientation with increasing discharge are statistically significant in four of the twelve digitised runs ($p < 0.05$; Kruskal-Wallis test). Changes in the distributions of patch elongation and area were only each statistically significant in one of the twelve runs ($p < 0.05$; Kruskal-Wallis test). There is no systematic relationship between how patch properties change as patches are eroded, and the composition of the sediment mixture.

The decrease in number of patches and consistent patch area suggest that as the primary erosion mechanism is the removal of entire patches, rather than patches becoming smaller through erosion round the edges. The change in patch orientation indicates some preferential erosion and local reworking, with grains being removed from patch flanks and deposited in downstream lee locations. The heterogeneity of patch behaviour demonstrates the influence of patch position relative to other

356 patches, with sediment from upstream erosion potentially resulting in simultaneous
357 accretion and erosion.

358 The interactions between sediment patches and local hydraulics will affect the spatial
359 distribution of grains across the bed. This distribution is quantified using Ripley's *L*
360 statistic. At one minute into the increase in discharge, variations in *L*(*r*) as a function
361 of spatial lag (Figure 7) show that at lags equivalent to one or two coarse grain
362 diameters, values of *L*(*r*) are significantly negative. Such values indicate that grains
363 are more dispersed than a random distribution. This is partly because the diameter
364 of the grains determines the minimum distance between grain centres, whereas in
365 the random simulations there is no minimum distance between points. The result
366 may also indicate that there is a minimum spacing between grains in the flume, i.e.
367 that grains are not in contact. For all sediment mixtures, at lags greater than about
368 three grain diameters, there is a rapid transition to significant positive *L*(*r*) values,
369 indicating clustering of the grains in patches.

370 The distribution of *L*(*r*) changes as the sediment patches are eroded (Figure 8 and
371 Figure 9); examples are shown from 100C/0F and 50C/50F, but the overall trends
372 are common to all runs. As the patches are eroded, *L*(*r*) starts to decrease. In run
373 100C/0F (Figure 8), sediment grains are randomly distributed by 20 minutes into the
374 increasing flow regime. Run 50C/50F, shows the same trend for reduced clustering,
375 although the values of *L*(*r*) are still above the simulated confidence interval at 25
376 minutes. The reduction in *L(r)* starts at the larger lags, indicating that grains are
377 becoming less clustered at this spatial scale, but retaining their clustering at smaller
378 scales. This suggests that the erosion of entire sediment patches dominates over
379 grain-by-grain erosion processes. If the latter process were dominant, *L*(*r*) would
380 decrease at smaller, as well as larger, lags. The interpretation of Figure 7, Figure 8

and Figure 9 is thus that there is clustering between the initial patches, but as erosion proceeds and patches are removed the spacing of the patches becomes more random. There are not, however, changes to the clustering of sediment grains within a patch.

4. Discussion

4.1. Controls on grain entrainment

Data from the three sets of experiments show that when sediment patches are present, the location of a grain in either an isolated or a patch position has a larger impact on the discharge at which it is entrained than does its diameter (Figure 3). The difference between isolated fine and coarse grains is far greater in the control experiments with single grains (Set 1) than in Set 3 when patches are present. Furthermore, the presence of patches also affects the discharge at which isolated grains are entrained, with isolated coarse grains being entrained at higher discharges in Set 2 than in Set 1 (Figure 2). This small but notable effect is evidence of the impact of sediment patches on hydraulic conditions across the measurement area. The impact of sediment patches is therefore twofold; grains in the patches have an increased critical shear stress through the combined effects of changed flow hydraulics and inter-grain friction, but isolated grains also have a reduced mobility as a result of the significant secondary effect of patches in changing the reach-scale hydraulics.

The impact of patch formation may be greater for the fine isolated grains, as expressed by the proportionally larger increase in discharge between Sets 1 and 3 because their size makes them more likely to be sheltered from the flow by upstream patches. The spatially variable pattern of shear stresses experienced by the isolated grains which results from the arrangement of other grains on the bed is displayed in

406 the difference between the minimum and mean discharges at which isolated grains
407 are entrained (Figure 3). In Set 3, isolated fine grains have the largest difference
408 between minimum and mean discharge, indicating that although many grains are
409 affected by the patches, some grains still occupy areas of the bed with similar
410 hydraulics to those in Set 1. For the coarse isolated grains and all patches, there is a
411 smaller, but notable, difference between the minimum and mean discharges,
412 indicating that there is a similar level of local shear stress variation within the patches
413 as there is in the areas surrounding them. Furthermore, the mean discharges are
414 similar in all locations, meaning that once the impact of grain geometry is accounted
415 for, the forces experienced by grains in a patch could actually be higher than those
416 experienced by isolated grains at the same discharge. This impact of the patch
417 geometry on the flow, and the overriding of grain size effects, is similar to that
418 observed in steep channels with immobile boulders by Yager *et al.* (2012), who also
419 found that sediment patch grain size was not always a good predictor of sediment
420 mobility. The experiments also show that the sediment composition had an impact
421 on the stability of fine and coarse patches, with patches being most stable when their
422 composition is most different to the bulk composition (e.g. fine patches are most
423 stable at 75C/25F). For fine grains, it follows that as the sediment coarsens, the
424 relative roughness of the bed will increase, and patches of fine sediment will become
425 relatively more sheltered. For coarse patches the phenomenon is harder to explain,
426 as coarse grains will become relatively more exposed as the sediment mixtures fine,
427 but may be related to the tendency of the finer sediment to form more numerous,
428 smaller, patches (Figure 5), which may more consistently increase roughness across
429 the entire measurement area.

430 ### 4.2. Sediment cover and patch geometry

As the sediment cover is eroded, sediment patches are removed through the erosion of discrete patches, and the distribution of patches across the bed becomes more random. There is also some evidence that patches become more elongate and aligned with the flow direction. The interaction between patches is constructive (Kocurek *et al*., 2010), and elements of merging, cannibalization and remote transfer are all seen in our experiments. However, our experiments are limited to short reaches and there is no upstream feed of sediment during erosion. Should a continuous feed, at a rate equal to the erosion rate from the observed reach, be introduced then regeneration and self-organisation of the bedforms may occur.

The form of the equilibrium between patch size, flow and sediment supply is likely to involve different bedform geometries under different boundary conditions (Nelson *et al.*, 2009; Dreano *et al.*, 2010; Hodge, in press), so cannot be predicted from present experiments. The process of patch removal suggests that patches may be sensitive to the entrainment of key grains, either in the patch or an upstream location, which change the local hydraulics and/or grain geometry. Positive feedback by which the erosion of grains destabilises surrounding grains means that a patch can be rapidly removed, as has been reported for particle clusters in alluvial rivers (Strom *et al.*, 2004; Tan and Curran, 2012; Heays *et al.*, 2014). Further analysis of the videos could attempt to identify the size and locations of these grains.

4.3. Feedbacks between flow and sediment patches

The development and erosion of sediment patches is a function of the feedbacks between flow, bed morphology and sediment transport (Werner, 2003; Kocurek *et al*., 2010). These experiments have demonstrated that under the idealised conditions in the flume, sediment patches can override the effects of grain size on grain entrainment, and can influence entrainment conditions in locations beyond the patch,

as well as within the patch itself. Consequently, the patches act to equalise the development and erosion of sediment cover across a range of sediment mixtures. The range of entrainment discharges demonstrated by both isolated and patch grains indicates that the patches induce spatial variation in flow conditions, both within and between the patches. As such these results provide some insight into the mechanisms by which patches self-organise, and provide physical support for rule-based models that have demonstrated the formation of such patches and other coarse bedforms (Werner and Fink, 1993; Hodge and Hoey 2010).

The observed impact of sediment patches on the critical grain entrainment discharge might suggest that with continual sediment supply, extensive sediment cover can rapidly develop as a result of runaway feedback mechanisms (Chatanantavet and Parker, 2008; Hodge and Hoey, 2010). Such cover does not occur in these experiments because of the limited duration and volume of sediment input. The erosion of sediment cover demonstrates the same mechanism in reverse, with rapid destabilisation of sediment patches. These mechanisms suggest that bedrock-alluvial rivers would tend to have binary sediment cover, with either limited or extensive cover, in the absence of larger-scale roughness elements that drive forced patch (bar) formation.

However, in these experiments, the bed developed a stable sediment cover of around 25% under the initial input conditions; the consistency between experiments in set 2 provides evidence that this was an equilibrium configuration. The development of this cover demonstrates that a relatively low spatial density of sediment grains is necessary to disrupt the hydraulics and create conditions suitable for the maintenance of that cover. This could suggest that under the limited and/or intermittent sediment supply common to many bedrock-alluvial rivers (Lague, 2010),

481 partial sediment covers may be common. This is further supported by the spatially
482 variable conditions induced by the sediment cover. The observed grain entrainment
483 will reflect the conditions of areas of the bed where grains were initially deposited,
484 i.e. those with lower flow velocities. The areas between the grains may be subject to
485 local flow acceleration as a result of grain blockages in other locations, which would
486 discourage deposition in these areas and the development of complete sediment
487 cover. Such preferential pathways for bedload transport have also been observed in
488 the field and flume under conditions of reduced sediment supply (Richardson *et al.*,
489 2003; Nelson *et al.*, 2009).

490 **4.4. Implications for bedrock-alluvial rivers**

491 These experiments demonstrate that even a relatively low density of sediment grains
492 can have a significant impact on flow hydraulics and sediment patch development.
493 Consequently, relatively small inputs of sediment into a channel could have notable
494 impacts on channel roughness, flow and sediment transport. The importance of the
495 development of patches will depend on the channel topography, with patches being
496 likely to have less of an impact in channels with a rougher bedrock topography
497 (Inoue *et al.*, 2014; Johnson, 2014). Under rough topographies, sediment patch
498 development could instead smooth the channel bed, producing a different set of
499 feedbacks. However, even within a channel with a grain-rough (*sensu* Inoue *et al.*,
500 2014) topography, there will still be areas of the bed that are locally flat at a scale
501 larger than that of the sediment grains, and in these locations the relationships these
502 experiments are likely to still apply.

503 These experiments have demonstrated that a single pulse of sediment can produce
504 a partial sediment cover. There are questions as to how this behaviour upscales to a
505 bedrock river with a fluctuating discharge and sediment supply. There are also

506 questions about the interactions between flow, sediment cover and sediment
507 entrainment under conditions of greater partial cover. The extent to which sediment
508 patches disrupt the flow is likely to be a non-linear process, with maximum disruption
509 occurring once a large proportion of the bed is affected by the wakes from patches.
510 As cover increases further, the bed will effectively become smoother again, reducing
511 the disruption.

512 These experiments also have implications for predicting sediment transport in
513 bedrock-alluvial rivers. The limited impact of grain size on grain entrainment in the
514 experiments with patches is consistent with previous observations that in channels
515 with partial sediment cover, sediment transport is independent of grain size (Hodge
516 *et al.*, 2011). In addition to potentially disregarding grain size, the experiments also
517 suggest that, in a mixture of isolated and patch grains, it may be appropriate to use a
518 single entrainment shear stress for both; however, this is not the case if the two
519 populations occur in distinct areas of the bed. The experiments do, however, suggest
520 that the magnitude of the critical shear stress will be a function of the extent of
521 sediment cover.

522 **5. Conclusions**

523 These experiments show that under idealised conditions (flat bed and maximum of
524 two grain sizes) the production and erosion of sediment patches on a flat surface is
525 affected by complex interacting processes. Isolated sediment grains away from the
526 influence of any other sediment are entrained at lower discharges than grains in
527 sediment patches. However, when sediment patches have formed in the flume,
528 isolated grains are entrained at a comparable mean discharge to grains in the
529 sediment patches. This is because of the influence of the sediment patches on the
530 local flow conditions.

The rate at which sediment patches are eroded as discharge is increased is approximately linear. The main reduction in sediment cover is through removal of entire patches, rather than grain-by-grain removal from patches. Sediment patches are reshaped as erosion progresses, becoming more flow orientated and sometimes more elongate. Grains are clustered at lags equivalent to a small number of grain diameters, but over time grain spacing at larger lags becomes more random.

Increasing understanding of the way in which sediment cover is produced and eroded on flat bedrock surfaces requires further research on the impact of sediment grains on the local flow, and consequent feedbacks on sediment transport processes. When there is an amount of sediment on the bed, these feedbacks appear to be the dominant control on patch stability, overriding the impact of grain size and whether grains are isolated or in a cluster.

Acknowledgements

Experiments in the hydraulics laboratory, University of Glasgow, had technical support from Stuart McLean, Tim Montgomery and Kenny Roberts, and additional help from Callum Pearson and Rebecca Smith. We thank that AE and two reviewers for their useful comments.

References

L'Amoreaux, P., and S. Gibson (2013), Quantifying the scale of gravel-bed clusters with spatial statistics, Geomorphology, 197, 56–63, doi:10.1016/j.geomorph.2013.05.002.

Carling P. A., Hoffmann M. and A. S. Blatter (2002). Initial motion of boulders in bedrock channels. In: Ancient Floods, Modern Hazards: Principles and Applications

555 of Paleoflood Hydrology, Water Science and Application Volume 5, pages 147-160,
556 AGU.

557 Carling P. A. and K. Tinkler (1998). Conditions for the entrainment of cuboid
558 boulders in bedrock streams: An historical review of literature with respect to recent
559 investigations. In: Rivers over Rock, AGU.Chatanantavet, P., and G. Parker (2008),
560 Experimental study of bedrock channel alluviation under varied sediment supply and
561 hydraulic conditions, Water Resour. Res., 44(12), doi:10.1029/2007WR006581.

562 Cressie, N.A.C. (1991) Statistics for Spatial Data, Wiley, New York.

563 Crocker, J.C., and D.G. Grier (1996), Methods of digital video microscopy for
564 colloidal studies, Journal of Colloid and Interface Science, 179(1) 298-310.

565 Dreano J., Valance A., Lague D. and C. Cassar (2010). Experimental study on
566 transient and steady-state dynamics of bedforms in supply limited configuration.
567 Earth Surf. Process. Landforms 35, 1730-1743, doi: 10.1002/esp.2085

568 Finnegan, N. J., L. S. Sklar, and T. K. Fuller (2007), Interplay of sediment supply,
569 river incision, and channel morphology revealed by the transient evolution of an
570 experimental bedrock channel, J. Geophys. Res., 112(F3),
571 doi:10.1029/2006JF000569.

572 Hajek, E. A., P. L. Heller, and B. A. Sheets (2010), Significance of channel-belt
573 clustering in alluvial basins, Geology, 38(6), 535–538, doi:10.1130/G30783.1.

574 Heays, K. G., H. Friedrich, and B. W. Melville (2014), Laboratory study of gravel-bed
575 cluster formation and disintegration, Water Resources Research, 50(3),
576 doi:10.1002/2013WR014208.

577 Hodge, R. A. (in press), Sediment processes in bedrock-alluvial rivers: Research
578 since 2010 and modelling the impact of fluctuating sediment supply on sediment
579 cover, Gravel Bed Rivers 8: Gravel Bed Rivers and Disasters, edited by J. Laronne
580 and D. Tsutsumi, Wiley.

581 Hodge, R. A., and T. B. Hoey (2012), Upscaling from grain-scale processes to
582 alluviation in bedrock channels using a cellular automaton model, Journal of
583 Geophysical Research: Earth Surface, 117, F01017, doi:10.1029/2011JF002145.

584 Hodge R. A., and T. B. Hoey (in revision), The impact of topography in a bedrock-
585 alluvial channel: 2. Sediment cover, J. Geophys. Res.,

586 Hodge, R. A., T. B. Hoey, and L. S. Sklar (2011), Bedload transport in bedrock
587 rivers: the role of sediment cover in grain entrainment, translation and deposition, J.
588 Geophys. Res., doi:10.1029/2011JF002032.

589 Inoue, T., N. Izumi, Y. Shimizu, and G. Parker (2014), Interaction among alluvial
590 cover, bed roughness and incision rate in purely bedrock and alluvial-bedrock
591 channel, J. Geophys. Res. Earth Surf., 2014JF003133, doi:10.1002/2014JF003133.

592 Johnson, J. P. L. (2014), A surface roughness model for predicting alluvial cover and
593 bed load transport rate in bedrock channels, J. Geophys. Res. Earth Surf.,
594 2013JF003000, doi:10.1002/2013JF003000.

595 Johnson, J. P. L., and K. X. Whipple (2010), Evaluating the controls of shear stress,
596 sediment supply, alluvial cover, and channel morphology on experimental bedrock
597 incision rate, J. Geophys. Res., 115, F02018, doi:201010.1029/2009JF001335.

598 Kocurek, G., Ewing, R.C. and D. Mohrig (2010), How do bedform patterns arise?
599 New views on the role of bedform interactions within a set of boundary conditions,
600 Earth Surf. Process. Landforms 35, 51–63, DOI: 10.1002/esp.1913

601 Krumbein, W. C. (1941) Measurement and geological significance of shape and
602 roundness of sedimentary particles. J. Sedimentary Research 11 (2), 64-72.

603 Lacey, R. W. J., and A. G. Roy (2008), The spatial characterization of turbulence
604 around large roughness elements in a gravel-bed river, Geomorphology, 102(3–4),
605 542–553, doi:10.1016/j.geomorph.2008.05.045.

606 Lague, D. (2010), Reduction of long-term bedrock incision efficiency by short-term
607 alluvial cover intermittency, J. Geophys. Res., 115, doi:10.1029/2008JF001210.

608 Lisle, T.E. (1995) Particle-size variations between bed-load and bed material in
609 natural gravel-bed channels, Water Res. Res. 31, 1107-18, doi:
610 10.1029/94WR02526

611 Nelson P. A., Venditte J. G., Dietrich W. E., Kirchner J. W., Ikeda H., Iseya F., and
612 L.S. Sklar (2009). Response of bed surface patchiness to reductions in sediment
613 supply. J. Geophys. Res. 114, F02005, doi: 10.1029/2008JF001144

614 Nelson, P. A., and G. Seminara (2012), A theoretical framework for the
615 morphodynamics of bedrock channels, Geophys. Res. Lett., 39, L06408,
616 doi:201210.1029/2011GL050806.

617 Papanicolaou, A. N., C. M. Kramer, A. G. Tsakiris, T. Stoesser, S. Bomminayuni,
618 and Z. Chen (2012), Effects of a fully submerged boulder within a boulder array on
619 the mean and turbulent flow fields: Implications to bedload transport, Acta Geophys.,
620 60(6), 1502–1546, doi:10.2478/s11600-012-0044-6.

621 Richardson K., Benson I. and P. A. Carling (2003). An instrument to record sediment
622 movement in bedrock channels. In: Erosion and Sediment transport measurement in
623 rivers: Technological and methodological advances (Proceedings of the Oslo
624 Workshop, June 2002). IAHS Publ. 283, 2003.

625 Seminara, G. (2010), Fluvial Sedimentary Patterns, *Annual Review of Fluid*
626 *Mechanics*, *42*, 43-66.

627 Siddiqui, A and Robert, A. (2010), Thresholds of erosion and sediment movement in
628 bedrock channels, Geomorphology, 118, 301-13, doi:
629 10.1016/j.geomorph.2010.01.011

630 Sklar, L. S., and W. E. Dietrich (2004), A mechanistic model for river incision into
631 bedrock by saltating bed load, Water Resources Research, 40, W06301,
632 doi:10.1029/2003WR002496.

633 Strom, K., A. N. Papanicolaou, E. Evangelopoulos, and M. Odeh (2004), Microforms
634 in Gravel Bed Rivers: Formation, Disintegration, and Effects on Bedload Transport,
635 Journal of Hydraulic Engineering, 130(6), 554–567, doi:10.1061/(ASCE)0733-
636 9429(2004)130:6(554).

637 Strom, K., and A. Papanicolaou (2007), ADV Measurements around a Cluster
638 Microform in a Shallow Mountain Stream, Journal of Hydraulic Engineering, 133(12),
639 1379–1389, doi:10.1061/(ASCE)0733-9429(2007)133:12(1379).

640 Tan, L., and J. Curran (2012) Comparison of turbulent flows over clusters of varying
641 density, Journal of Hydraulic Engineering 138 (12), 1031-1044.

642 Turowski, J. M., N. Hovius, A. Wilson, and M.-J. Horng (2008), Hydraulic geometry,
643 river sediment and the definition of bedrock channels, Geomorphology, 99), 26–38,
644 doi:10.1016/j.geomorph.2007.10.001.

645 Turowski, J. M., D. Lague, and N. Hovius (2007), Cover effect in bedrock abrasion: A
646 new derivation and its implications for the modeling of bedrock channel morphology,
647 J. Geophys. Res., 112(F4), doi:10.1029/2006JF000697.

648 Werner B.T. (2003), Modeling landforms as self-organized, hierarchical dynamical
649 systems. In Prediction in Geomorphology, Wilcock PR, Iverson RM (eds).
650 Geophysical Monograph 135, American Geophysical Union: Washington; 133–150

651 Werner, B. T., and T. M. Fink (1993), Beach cusps as self-organized patterns,
652 Science, 260(5110), 968–971.

653 Wohl, E.E. (2015), Particle dynamics: the continuum of alluvial to bedrock river
654 segments, Geomorphology 241, 192-208, doi:10.1016/j.geomorph.2015.04.014
655

Experimental property	**Set**		
	1	**2**	**3**
Sediment mixtures	Single grains C and F	100C	100C, 75C/25F, 50C/50F, 25C/75F, 10C/90F & 100F
Sediment size(mm)	Coarse = 15	Coarse = 15	Coarse = 15

	Fine = 8.5		Fine = 8.5
Sediment mass supplied per run (kg)	single grain	20	6
Bed slope	0.0067	0.0050	0.0067
Flow rate during patch development (l s^{-1})	n/a	7.5 – 8.5	8.8
Flow depth (mm)	9 – 20 (F) 15 – 35 (C)	~30 (input) ~ 50 – 80 (final erosion)	~ 20 – 40 (input) ~ 50 – 80 (final erosion)
Time for sediment cover to develop (min)	n/a	~15	~15
Time for erosion (min)	n/a	~30	~30
Number of repeats	Coarse: 25 Fine: 25	21	100F: 5 100C & 10C/90F: 3 Others: 4

656 Table 1: Properties for the experimental runs.

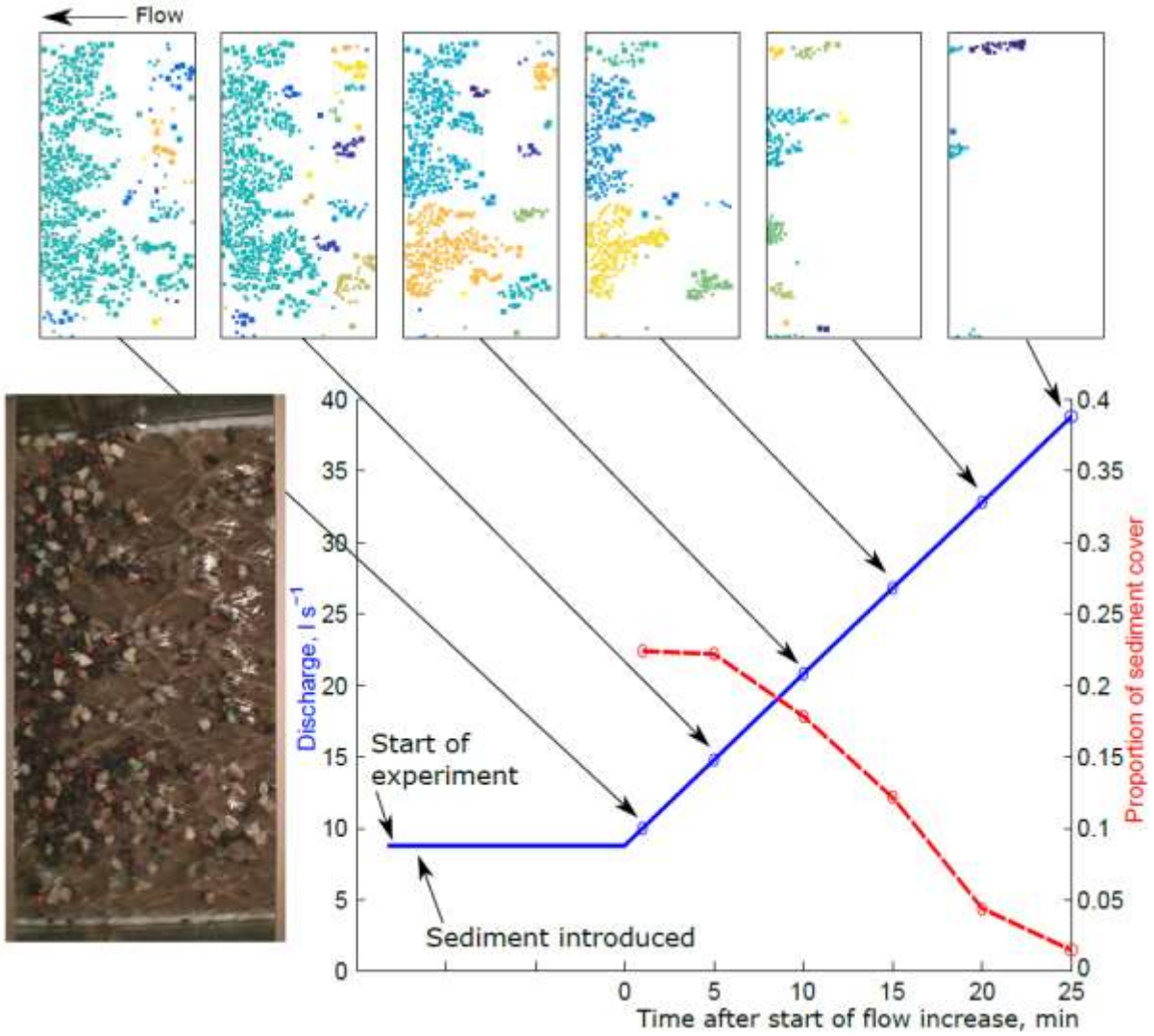

Figure 1: Outline of the experimental procedure used in all experiment runs. In Set 1, individual grains were introduced, whereas in Sets 2 and 3 volumes of sediment were added. Insets show examples of digitised grains, taken from video stills of the measurement area. A patch is defined such that all grains in a patch are less than one grain diameter from a neighbouring grain. Different patches are shown with different colours, but colours are not consistent between time periods. Video stills and proportion of sediment cover data are from a 50C/50F run. The inset photo is of the bed at 1 minute into the increase in flow.

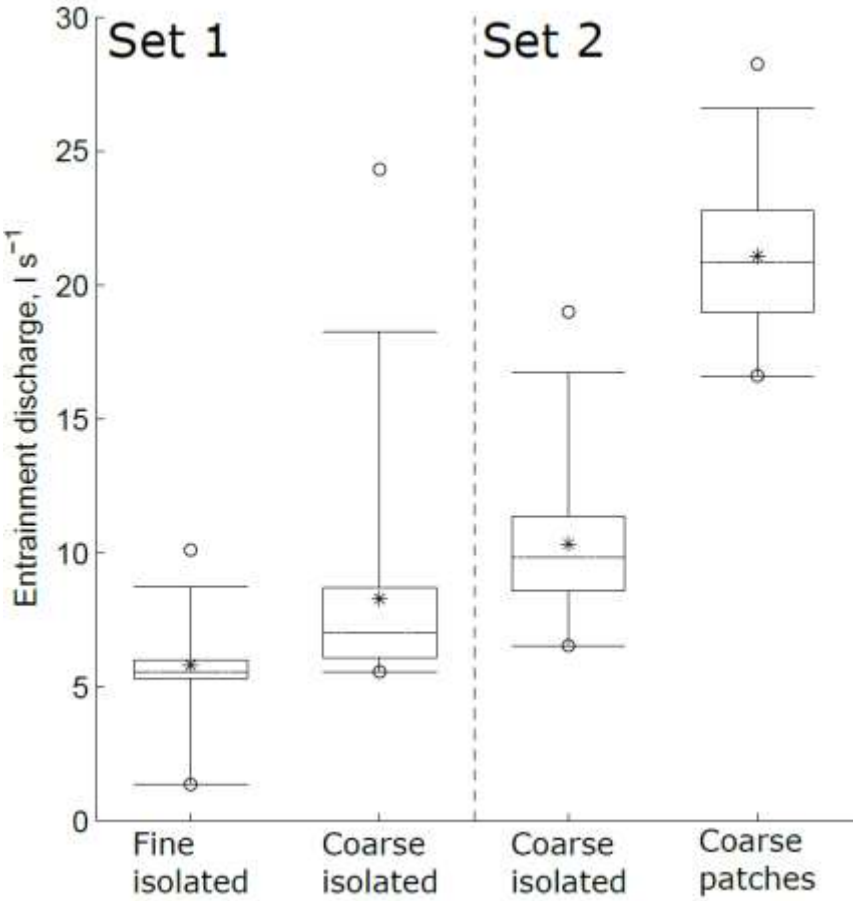

Figure 2: Distributions of discharges at which grains in Set 1 (n=25) and Set 2 (n=21) experiments were entrained. Set 1 consisted of individual grains, whereas Set 2 comprised a mixture of isolated grains and sediment patches. For Set 2, the discharge is that at which sediment started moving. Whiskers show 5th and 95th percentiles, circles show minimum and maximum, and stars show mean. In Set 1 the difference in entrainment discharge between fine and coarse grains is statistically significant (t-test, 0.007), as is the difference between coarse isolated and coarse patch grains in Set 2 (t-test, $p < 0.0001$). The difference between the entrainment discharge for coarse isolated grains in Set 1 and Set 2 is not statistically significant (t-test, $p = 0.057$).

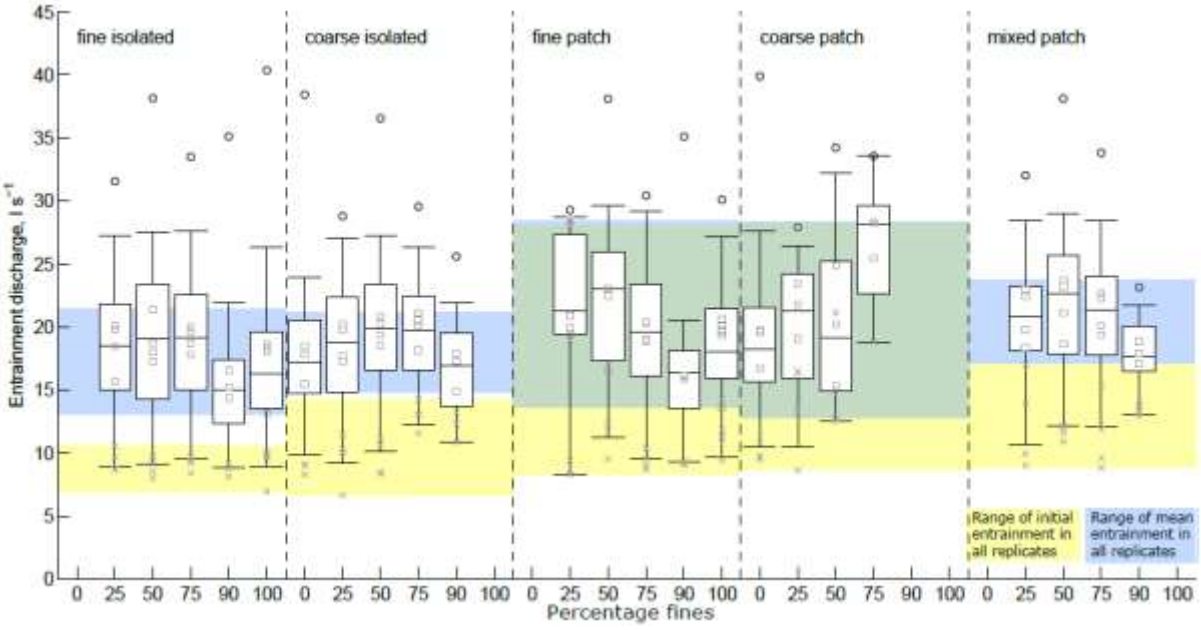

Figure 3: Distributions of discharges at which grains were entrained in Set 3 experiments. Data are grouped by sediment mixture, and grain size and location. The box plots show the combined data from all replicates with that sediment mixture. Whiskers show 5th and 95th percentiles, and black circles show maximum. Grey crosses and squares respectively show minimum and mean values from individual replicates; there is more variability for sediment in patches than for individual grains. The Kruskal-Wallis test indicates a significant difference ($p < 0.05$) between the minimum discharges for different grain sizes and positions in runs 100C/0F, 10C/90F, 50C/50F and 25C/75F. The Kruskal-Wallis test also shows that, for each sediment mixture, there are significant differences between the full distributions of entrainment discharges for grains in different locations ($p \leq 0.02$).

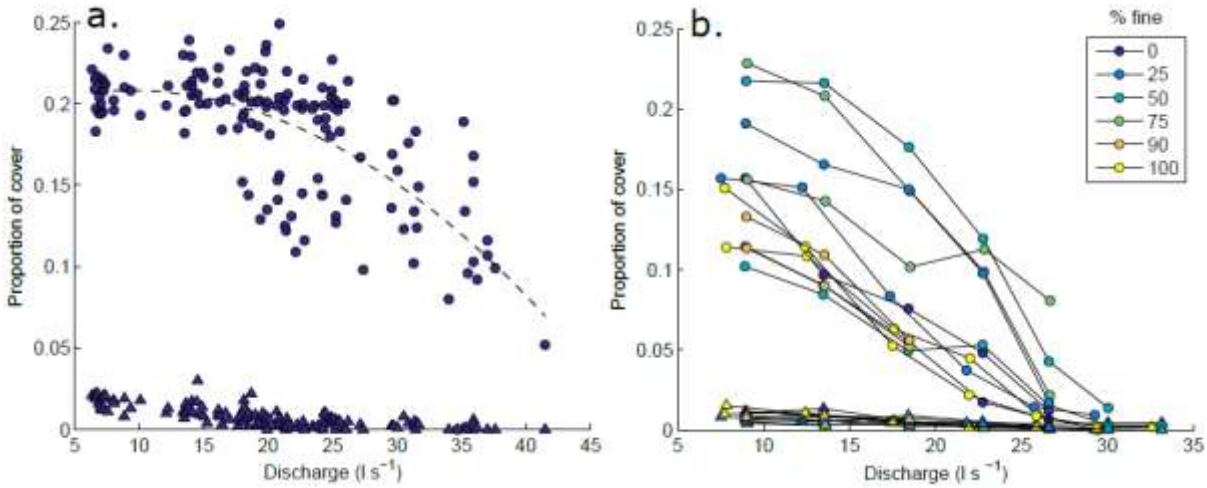

689

690 Figure 4: Decrease in sediment cover with increasing discharge for experiments in a)
691 Set 2 and b) Set 3. In both, circles are cover from patches and triangles are cover
692 from isolated grains. Dashed line in a) shows a polynomial fit to the patch data.

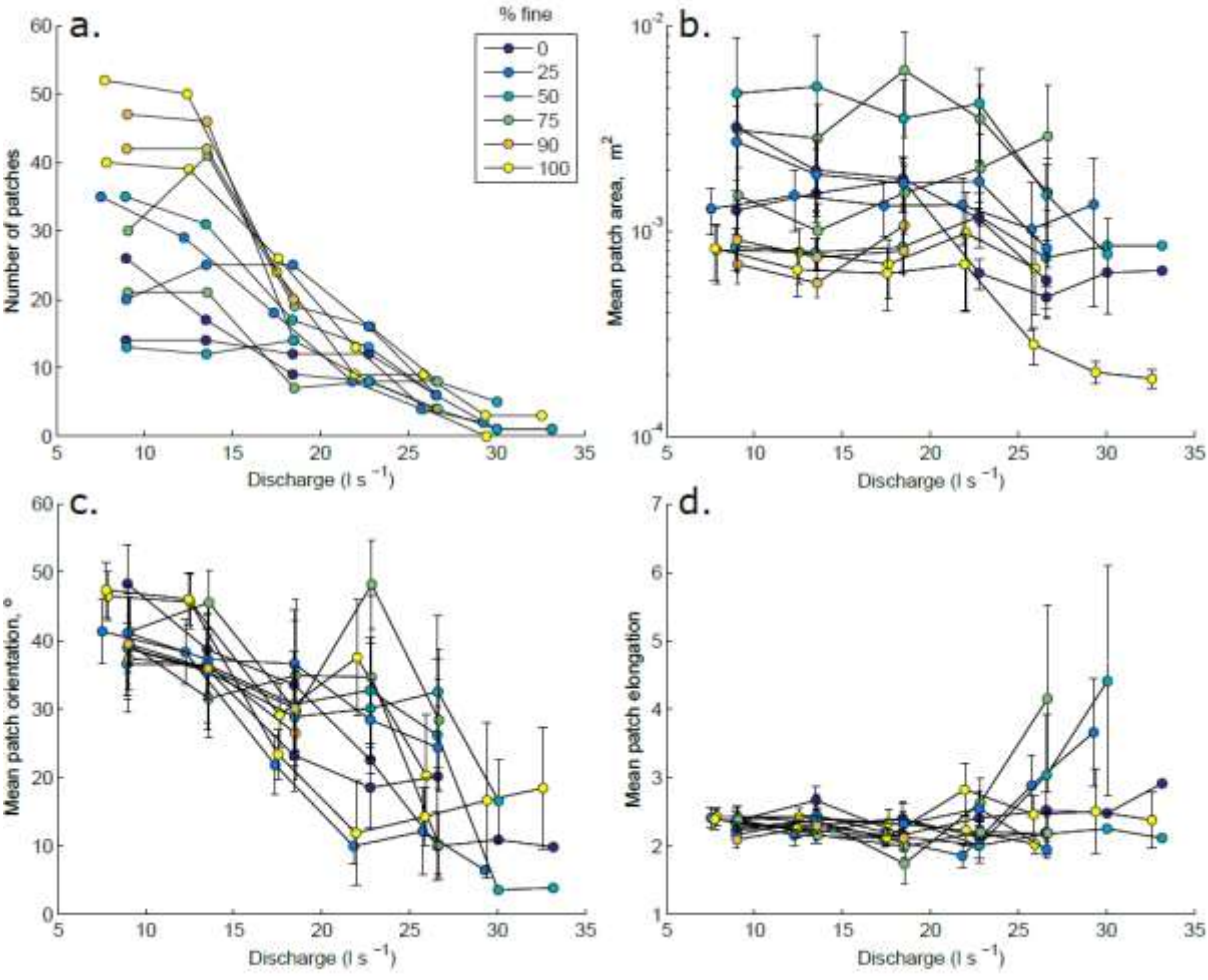

693

Figure 5: a) Number of patches, b) mean patch area, c) orientation and d) elongation as a function of changing discharge for selected Set 3 experiments. Orientation is measured relative to the downstream direction: 90° is perpendicular to flow and 0° parallel to flow. Area is the total bed area containing all the patch grains, not just the area of the grains themselves, and so includes areas of exposed bed within the patch outline. Elongation is the ratio of the lengths of patch major to minor axes. Error bars are one standard error of the mean.

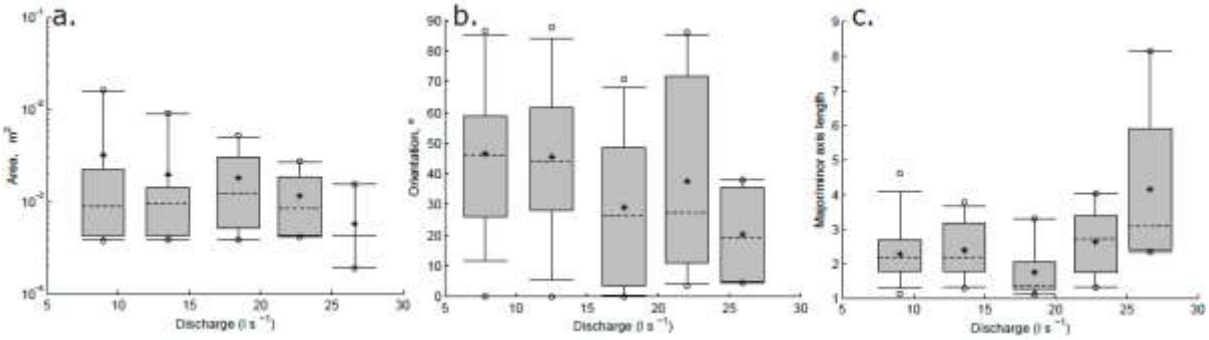

Figure 6: Examples of the changes in patch properties as a function of increasing discharge. In a. and b. there is a significant difference between the distributions (Kruskal-Wallis, $p < 0.05$). c. shows a representative example, but the differences are not significant.

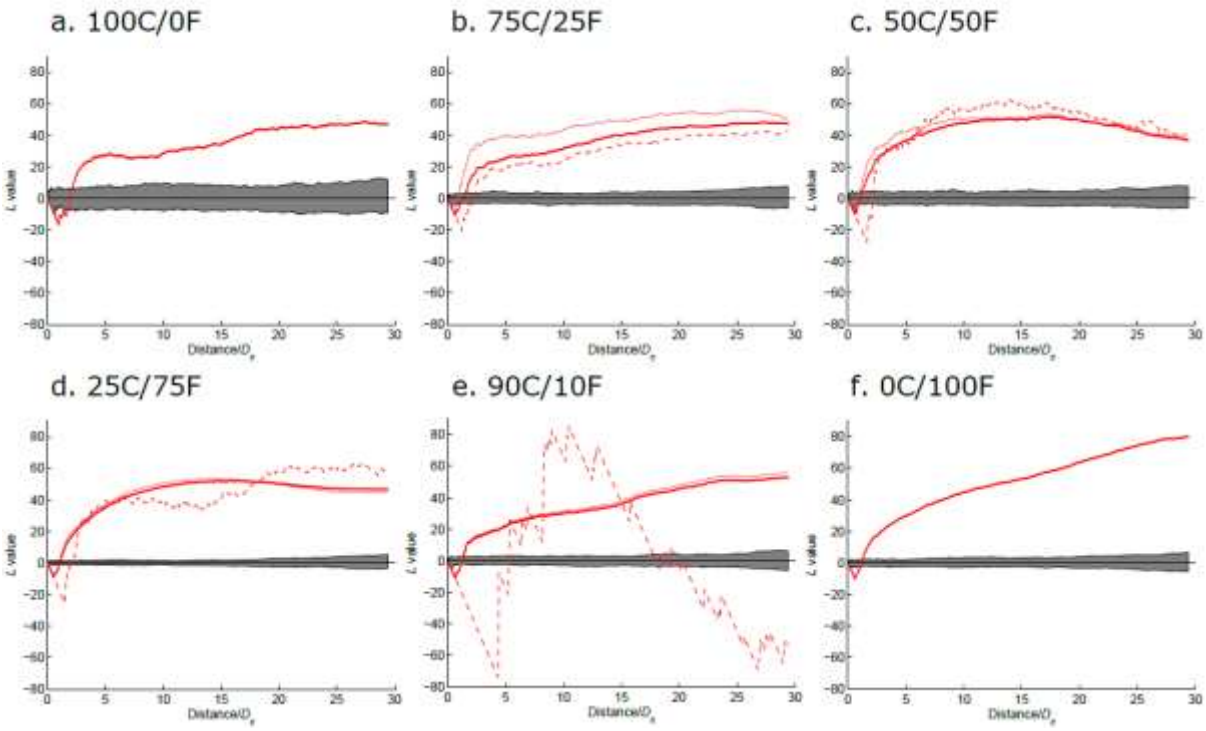

Figure 7: Values of Ripley's *L* at increasing spatial lags for the sediment grain distributions one minute into the flow increase. Values greater than zero indicate greater clustering than random, and values less than zero indicate greater dispersion than random. Solid line is for all grains. Fine line with short dashes is just fine grains, fine line with large dashes is just coarse grains. Grey areas are a 95% confidence interval, calculated from 100 repeat simulations with random spacing of n grains (where n is the number of digitised grains). Grain diameter (D_c) is the coarse grain diameter in all cases.

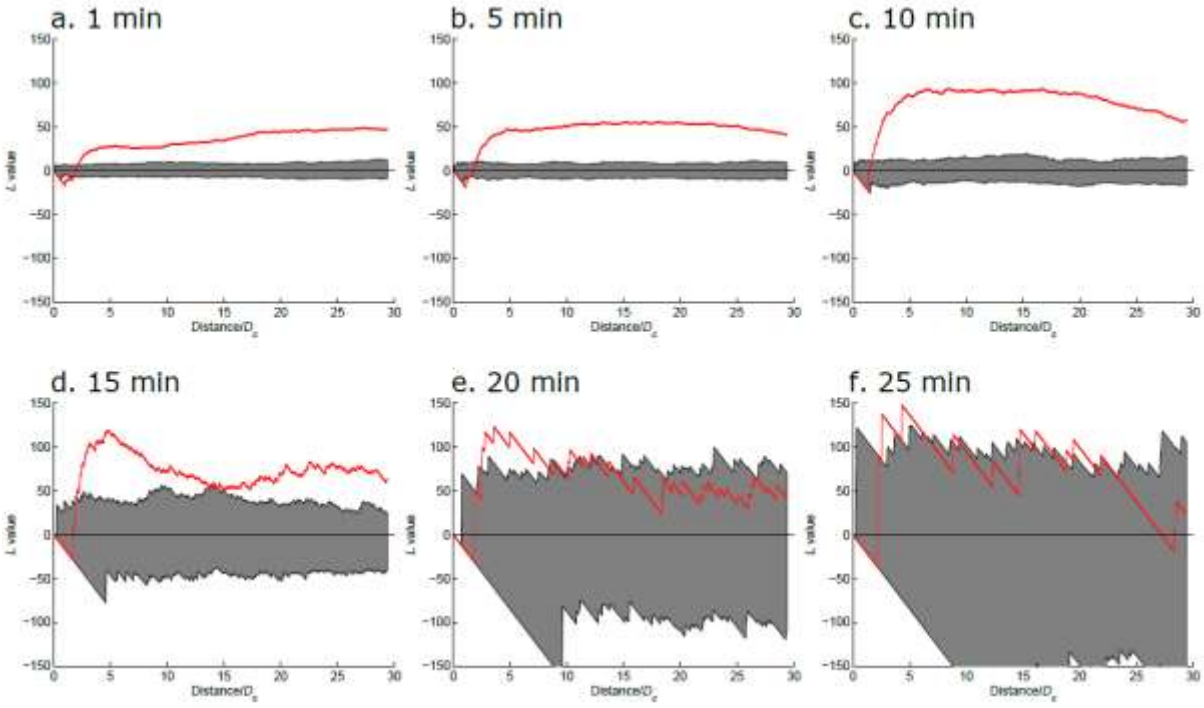

715

716 Figure 8: Values of Ripley's *L*(*r*) at increasing spatial lags for the sediment grain
717 distributions at increasing discharge in run 100C/0F. See caption of Figure 7 for
718 further information.

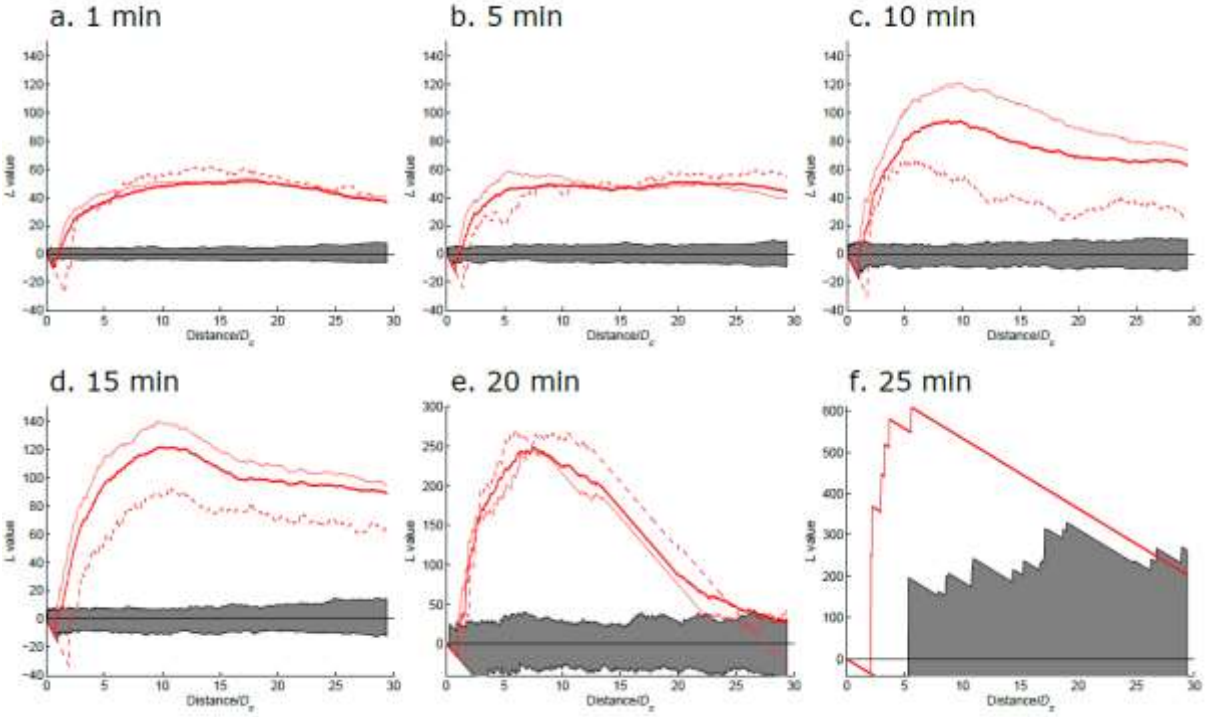

719

720 Figure 9: Values of Ripley's *L*(*r*) at increasing spatial lags for the sediment grain
721 distributions at increasing discharge in run 50C/50F. See caption of Figure 7 for
722 further information. Note different vertical axis scales in e. and f.

723